

Deciphering Blazar Emission Zones through Polarisation and Spectral Energy Distribution Studies

Hester M. Schutte, Markus Böttcher

Collaborators: Justin Cooper, Brian van Soelen and David A. H. Buckley

Conference **HIGH-ENERGY ASTROPHYSICS IN SOUTHERN AFRICA**



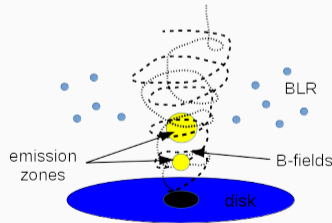
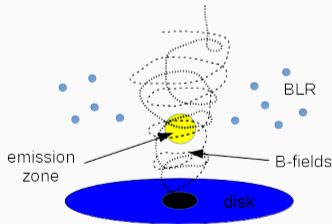
Wits Rural Facility, South Africa

2-4 October 2024

Introduction: Three Different Types of Emission Zones Models (Time-Independent and Leptonic)

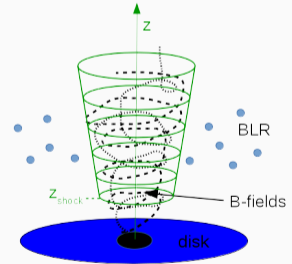
One and Two Emission Zone Models

Böttcher et al., 2013; Zhang & Böttcher, 2013



Multiple Domains

Tavecchio et al., 2018



Introduction: Leptonic Model

ELECTRON DISTRIBUTION

Broken power-law with
exponential cut-off $\Rightarrow F_{\omega}^{syn}$

SYNCHROTRON POLARISATION

Rybicki and Lightman, 1979

$$\Pi^{sy} = F_B \cdot \frac{\langle G(x) \rangle}{\langle F(x) \rangle}$$

$$\langle G(x) \rangle = \int N_e(\gamma) x(\gamma) K_{2/3}(x(\gamma)) d\gamma$$

$$\langle F(x) \rangle = \int N_e(\gamma) x(\gamma) \int_{x(\gamma)}^{\infty} K_{5/3}(x(\psi)) d\psi d\gamma$$

ACCRETION DISK

(Shakura and Sunyaev, 1973)
Assuming a thin disk and
non-rotating BH.

BLR EMISSION LINES

Approximated as Gaussians



Thermal emission is expected to
be unpolarised and due to the
approximate azimuthal symmetry
 \Rightarrow unpolarised EC emission.

INVERSE COMPTON RADIATION Böttcher et al., 2012

$$j_\nu(\epsilon_s, \Omega_s) \propto \int d\gamma n_e(\gamma) \int d\Omega_{ph} \int d\epsilon n_{ph}(\epsilon, \Omega_{ph}) \frac{d\sigma_C}{d\epsilon_s}$$

SSC

Bonometto and Saggion,
1973

$$\Pi_\omega^{SSC} = \frac{P_\omega^{SSC, \perp} - P_\omega^{SSC, \parallel}}{P_\omega^{SSC, \perp} + P_\omega^{SSC, \parallel}}$$

ACCRETION DISK

SEED PHOTONS

(Böttcher et al., 1997)

Depends on disk intensity
and angle at which photon
travels from disk.

BLR SEED PHOTONS

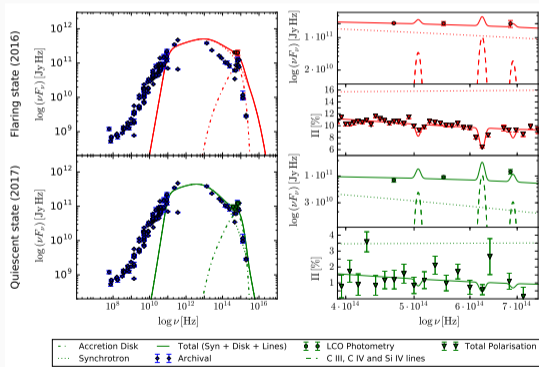
(Böttcher et al., 2013)

Modelled as an isotropic
thermal photon field in the
AGN rest frame.

TOTAL DEGREE OF POLARISATION: $\Pi_\omega^{Total} = \frac{\Pi_\omega^{SSC} \cdot F_\omega^{SSC} + \Pi^{sy} \cdot F^{sy}}{F_\omega^{sy} + F_\omega^d + F_\omega^{em.lines} + F_\omega^{SSC} + F_\omega^{EC}}$

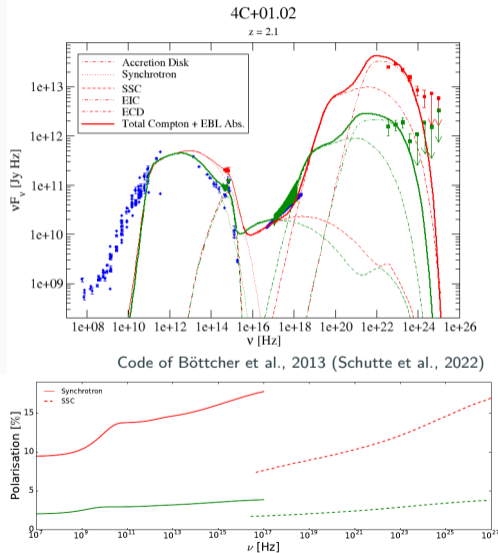
One Zone Leptonic Model for 4C+01.02

Polarisation diluted by thermal components:
accretion disk and BLR



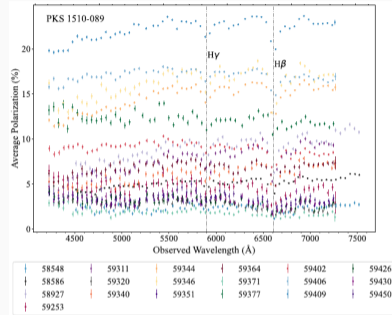
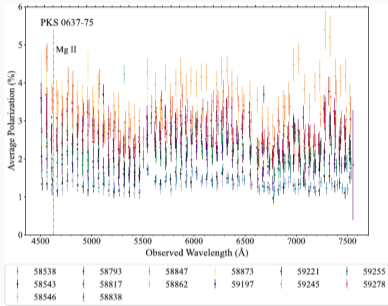
Constrains $F_B < 1$: $F_B^{\text{flare}} = 0.2$, $F_B^{\text{quies}} = 0.04$ and $M_{BH} = 5 \times 10^9 M_\odot$.

Schutte et al., 2022



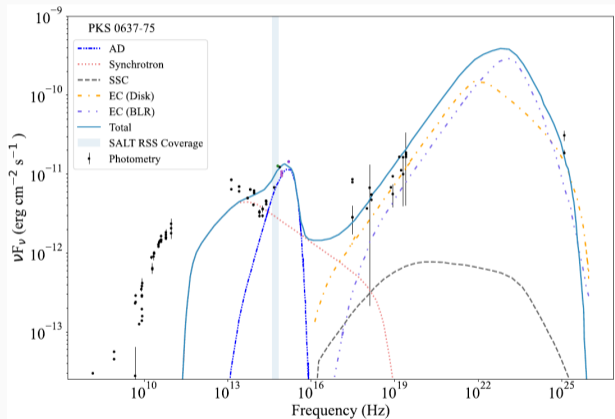
SSC polarisation - code of Zhang and Böttcher, 2013

Unpolarised Emission Lines in PKS 1510 - 089 and PKS 0637 - 75



Non-detection of polarisation in broad emission lines, in agreement with predictions by Oudmaijer & Harries, 2008; Capetti et al., 2021 \Rightarrow polarised emission undergo geometric cancellations due to the pole-on orientation.

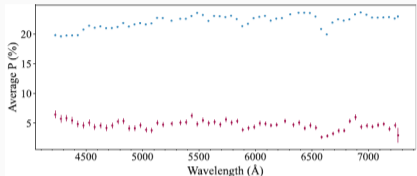
One Zone Leptonic Model for PKS 0637 - 75



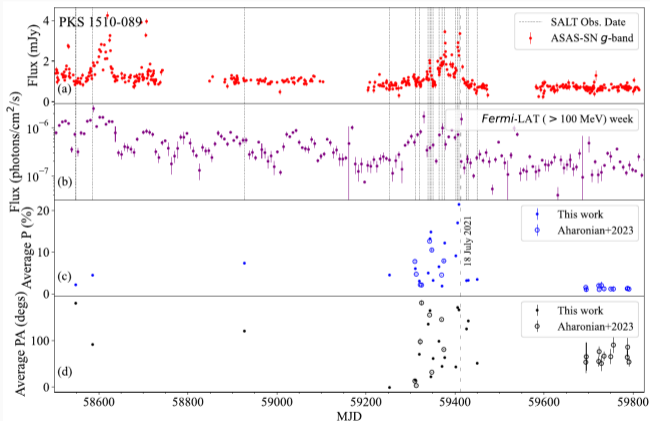
Modelling with Böttcher et al. (2013) code.

- Indicative of dominating disk.
- Emission region located 0.06 pc down the jet, within the BLR, \Rightarrow dominant external Compton contributions from the disk and BLR

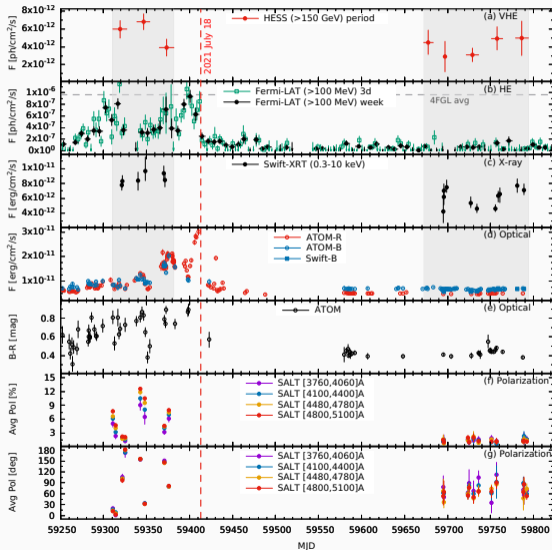
Changing Phenomena Observed in PKS 1510 - 089



- Polarisation change from optical quiescent (MJD 59253, red) to flaring (MJD 59409, blue) periods of PKS 1510 - 089.
- Thermal \rightarrow non-thermal emission dominance.



Two Emission Zones: PKS 1510-089



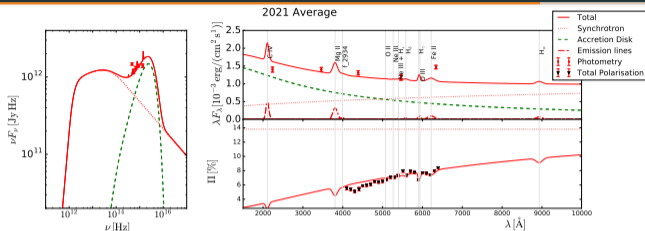
In 2021 July: sudden and significant decrease in:

- high-energy fluxes (*Fermi*-LAT)
- optical fluxes (*Swift*-UVOT, ATOM)
- optical polarization (SALT)

however, the following fluxes remained relatively steady:

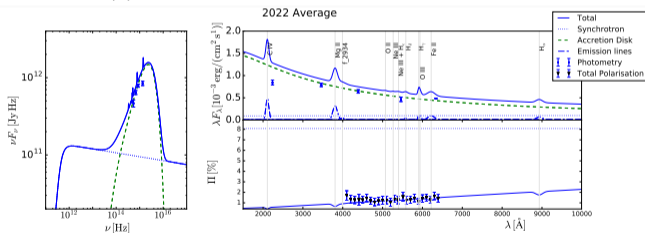
- very high-energy gamma-ray (H.E.S.S.)
- X-ray, *Swift*-XRT

Two Emission Zones, PKS 1510-089: Disappearing optical polarization



Fitting the optical/UV fluxes and averaged polarisation data of 2021 and 2022.

2021: Contribution from accretion disk and synchrotron radiation



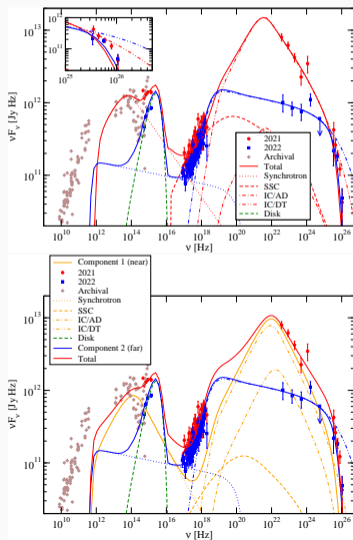
2022:

- Photometry data can be fitted with disk component (excl. syn.)
- Polarisation degree almost zero %
⇒ dominating disk contribution.
- Polarisation observed ⇒ ISM (% received from comparison star).
⇒ Upper limit synchrotron polarisation.

Ave.	p_2	B-field ordering, F_B	χ^2_{pol}/ndf
2021	3.7	0.18	0.06
2022	3.1	0.1	0.10

$$M_{BH} = 6 \times 10^8 M_{\odot}, L_{disk} = 1.8 \times 10^{46} \text{ erg s}^{-1}, \text{ Spectropol. data d.o.f. } ndf = 13$$

Two Emission Zones, PKS 1510-089: Extending Results to the Broadband Spectral Energy Distribution



Resulting parameters implemented in the leptonic model of Böttcher et al., 2013:

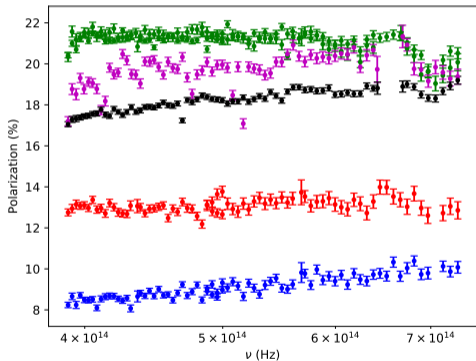
Parameter	2021	2022	2021
[units]	single-zone	single-zone	two-zone
R [cm]	3.0×10^{15}	1.0×10^{16}	5.0×10^{15}
B [G]	2.0	2.0	2.2
z_0 [pc]	0.1	10	0.06

$$\Gamma = 20, \theta_{\text{obs}} = 2.9 \text{ deg}, u_{\text{ext}} = 1.5 \times 10^{-3} \text{ erg cm}^{-3}$$

Top figure: One-zone model fits.

Bottom figure: Two-zone model fits. The primary emission zone within the BLR \Rightarrow synchrotron and HE γ -ray radiation. Secondary zone, located 1 pc from the black hole, produces X-ray and VHE γ -ray.

Observations Supporting Multiple Domains Model: 3C 279



SALT Spectropolarimetry

- The magnetic field ordering decreases in each domain along the jet.
- Higher ordered magnetic fields (or B_{\perp}) and higher energy particles are found near the shock regime.
As the magnetic field becomes less ordered, particles cool down along the jet.
- Trend for IXPE observed HBLs (Di Gesu et al, 2023; Liodakis et al., 2023;).

The amount of emission zones required in a model is dependent on the regions where the jet is active.

- A one-zone model cannot describe radiation from all sources. It can sufficiently describe the observations from 4C +01.02 and PKS 0637 -75.
- A two-zone model is required to fit PKS 1510 - 089 as determined from the spectral energy distribution.
- The multiple domain model is required to fit 3C 279 as seen from degree of polarisation data.



Thank you!



National
Research
Foundation

Appendices

Observations: SALT ToO Program "Observing the Transient Universe"

The SALT ToO Program "Observing the Transient Universe" (PI: D.A.H. Buckley) conducts spectropolarimetry and spectroscopy observations of blazars and contemporaneous observations are included from the LCO (PI: Brian van Soelen) and the Steward Observatory, *Fermi*-LAT and the *Swift*-XRT (when available).

- 20 blazars observed (16 FSRQ, 3 BL Lacs, 1 blazar candidate of unidentified classification)
- redshifts of 0.1 to 2.1
- Multi-epoch observations for 10 blazars
- Polarisation degrees of 0 to ~ 30 %

In this presentation we will be focussing on: 4C+01.02, 3C 273 and 3C 279

One Zone Leptonic Model: Low-Energy Components

ELECTRON DISTRIBUTION

Broken power-law with exponential cut-off

SHAKURA AND SUNYAEV (1973) ACCRETION DISK

Assuming a thin disk ($L_d < 0.3L_{Edd}$) and non-rotating BH.

The peak of the accretion disk component corresponds to the maximum disk temperature at the inner disk radius:

$$\nu^d(T^{max}) \propto M_{BH}^{-1/4}$$

BLR EMISSION LINES

- Approximated as Gaussians.
- Flux heights (independent of the continuum flux) relative to each other (Francis et al., 1991).

SYNCHROTRON POLARISATION According to Rybicki and Lightman (1979):

$$\begin{aligned}\Pi^{sy} &= F_B \cdot \frac{\langle G(x) \rangle}{\langle F(x) \rangle} \\ \langle G(x) \rangle &= \int N_e(\gamma) x(\gamma) K_{2/3}(x(\gamma)) d\gamma \\ \langle F(x) \rangle &= \int N_e(\gamma) x(\gamma) \int_{x(\gamma)}^{\infty} K_{5/3}(x(\psi)) d\psi d\gamma\end{aligned}$$

TOTAL LOW-ENERGY DEGREE OF POLARISATION: $\Pi^{total} = \frac{\Pi^{sy} \cdot F^{sy}}{F^{sy} + F^d + F^{em.lines}}$

One Zone Leptonic Model: High-Energy Components

INVERSE COMPTON RADIATION (Böttcher et al., 2012):

$$j_{\nu}^{\text{head-on}}(\epsilon_s, \Omega_s) \propto \int d\gamma n_e(\gamma) \int d\Omega_{ph} \int d\epsilon n_{ph}(\epsilon, \Omega_{ph}) \frac{d\sigma_C}{d\epsilon_s}$$

BLR SEED PHOTONS (Böttcher et al., 2013): Modelled as an isotropic thermal photon field in the AGN rest frame.

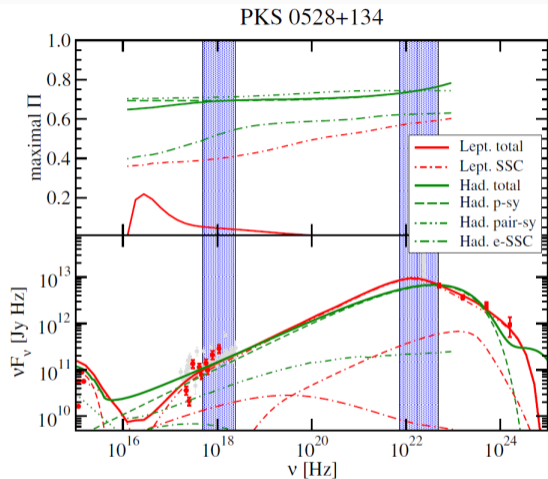
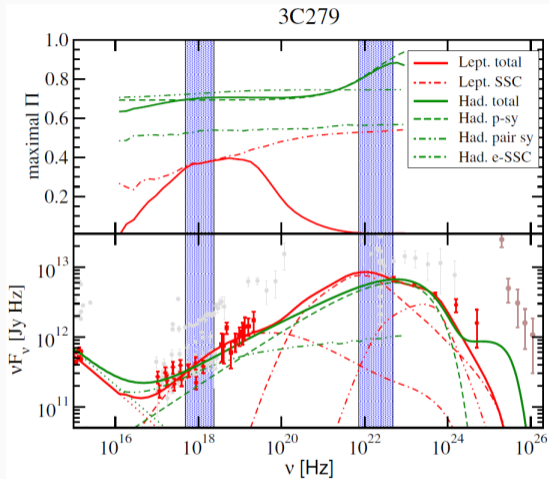
ACCRETION DISK PHOTON DISTRIBUTION (Böttcher et al., 1997): depends on disk intensity and angle at which photon travels from disk.

EC emission is expected to be unpolarised due to the approximate azimuthal symmetry and unpolarised target photons.

SSC POLARISATION (Bonometto and Saggion, 1973):

$$\Pi_{\omega}^{SSC} = \frac{P_{\omega}^{SSC, \perp} - P_{\omega}^{SSC, \parallel}}{P_{\omega}^{SSC, \perp} + P_{\omega}^{SSC, \parallel}}$$

TOTAL HIGH-ENERGY DEGREE OF POLARISATION: $\Pi_{\omega}^{SSC} = \frac{\Pi_{\omega}^{SSC} \cdot F_{\omega}^{SSC}}{F_{\omega}^{SSC} + F_{\omega}^{EC}}$



$$F_B = 1$$

Zhang and Böttcher (2013)

- **Degree of polarisation decreasing towards optical-UV frequencies:** Can be described by a one zone leptonic model wherein thermal components dilute non-thermal synchrotron polarisation. However, according to the shock in jet model, magnetic field ordering decreases along the downstream jet:
- **Degree of polarisation increasing towards optical-UV frequencies** wherein we expect well-defined polarisation close to the shock regime (high B_{\perp}) - electrons emitting at X-ray energies. At lower (optical-IR) frequencies, lower energy electrons experience a less ordered magnetic field, yielding the lower polarisation degree observed in the optical regime.

Spectropolarimetry allows for disentanglement of radiation components (thermal vs. non-thermal) and understanding the ordering of the magnetic field along the jet, thereby, enabling the constraint of SSC polarisation to model IXPE observations. This can also contribute to distinguish between leptonic and hadronic models.